Supporting Information

Nitridation-Driven Construction of Ru/WNO Catalysts Enables Highly Selective Cellulose to C_2 Alcohols Hydrogenolysis

Wei Jia[a], Nianxue Zhai[b], Hongxiao Wang[b], DanDan Wang[b], Yuandong Cui[b], Guoqing Ren[c,*], Xiaoli Yang[b,*]

[a] Pei County Secondary Specialized School of Jiangsu Province, Xuzhou 221600, China

[b] College of Textiles and Clothing, State Key Laboratory of BioFibers and Eco-textiles, Qingdao University, Qingdao 266071, China

[c] Institute of Frontier Chemistry, School of Chemistry and Chemical Engineering, Shandong University, Qingdao, Shandong, 266237, P. R. China

* Corresponding author. Email: renguoqing@sdu.edu.cn, xlyang@qdu.edu.cn

No of Pages: 14

Summary:

Experimental Section

Reference

Experimental Section

Materials and catalyst preparation

Tungsten chloride (WCl_6), absolute ethanol (99.7%), microcrystalline cellulose (25 μm), ethylene glycol (98%), glucose (99%), fructose (99%), sorbitol (98%), mannose (99%), propylene glycol (99%), and butylene glycol (98%) were purchased from Shanghai Aladdin Biochemical Technology Co., Ltd., and all chemicals were used without further processing. Ruthenium (III) chloride hydrate ($RuCl_3 \cdot xH_2O$, ReagentPlus®) was purchased from Merck KGaA, Darmstadt, Germany. Before use, it was dissolved in deionized water and diluted to a concentration of 10 g L^{-1}.

WO_x was synthesized by dissolving 1.6 g of WCl_6 in 80 mL of ethanol and stirring for 30 min until a dark-blue solution was obtained. The mixture was then transferred to a PTFE-lined autoclave and heated at 160 °C for 12 h. The resulting solid was filtered, washed thoroughly with deionized water, and dried under vacuum to afford blue WO_x. Nitridation was performed in a tubular furnace under flowing NH_3 at 400, 600, 800, or 900 °C (2 h, 5 °C min^{-1}), yielding WNO-*t* (*t* = nitridation temperature).

Ru/WNO-*t* catalysts were prepared by incipient wetness impregnation. Typically, 200 mg of WNO-*t* was dispersed in 50 mL of deionized water, followed by addition of an appropriate volume of $RuCl_3$ solution to achieve 3 wt% Ru loading. After stirring for 2 h, the mixture was dried, ground, and reduced under H_2 at 400 °C for 2 h. The reduced samples were passivated in 1% O_2/N_2 for 2 h (5 °C min^{-1}) to obtain the final catalysts.

Catalytic activity measurements

Catalytic tests were conducted in a 100 mL stainless-steel autoclave. A mixture of catalyst (50 mg), microcrystalline cellulose (100 mg), and deionized water (30 mL) was loaded into the reactor. After sealing, the system was purged with H_2 several times, then pressurized to 5 MPa with high-purity hydrogen (99.999%). The reaction was carried out at 245 °C for 4 h under magnetic stirring (600 rpm). Notably, at an initial pressure of 5 MPa, the pressure inside the vessel reaches 10.2 MPa when the reactor is heated to 245 °C. After cooling to room temperature, the liquid products were analyzed by HPLC (Agilent 1260) equipped with an 87-H column and a refractive index detector (RID). A 2 mmol L^{-1} H_2SO_4 aqueous solution was used as the mobile phase at 0.6 mL min^{-1}. All catalytic tests were repeated three times, and the relative error for each sample was controlled within 3%. Carbon balance was calculated based on quantified liquid-phase products. Under the optimized conditions used for

catalyst comparison, the carbon balance exceeded 90%, whereas lower values were observed at incomplete conversion due to the formation of undetected oligomeric species.

Catalysis characterization

X-ray diffraction (XRD) patterns were recorded on a Rigaku Ultima IV diffractometer using Cu Kα radiation (λ = 0.15406 nm) with a scanning rate of 10°·min^{-1} over a 2θ range of 10°-80°. Scanning electron microscopy (SEM) images were acquired on a Sigma 500 microscope. Transmission electron microscopy (TEM) analysis was carried out using a Talos F200SG2 microscope to examine particle size and lattice structure.

Brunauer-Emmett-Teller (BET) specific surface area was measured using a TriStar 3000 analyzer after degassing samples at 120 °C for 3 h. X-ray photoelectron spectroscopy (XPS) was conducted on a PHI 5000 VersaProbe II spectrometer, and binding energies were calibrated to the C 1s peak at 284.8 eV. Raman spectra were collected on a Thermo Fisher DXR2 micro-Raman spectrometer.

NH_3 temperature-programmed desorption (NH_3-TPD) measurements were performed on a MICROTRAC MRB BELCAT-II apparatus. Samples were first pretreated in Ar at 250 °C (5 °C min^{-1}, 1 h), then reduced in 5 vol% H_2/Ar by heating to 400 °C (5 °C min^{-1}, 30 min). After cooling to 50 °C and purging with Ar, adsorption of 5 vol% NH_3/Ar was carried out until saturation. The samples were subsequently purged with Ar to remove weakly adsorbed species, followed by temperature-programmed desorption from 50 °C to 900 °C at 10 °C min^{-1} under Ar flow.

Pyridine-adsorbed FTIR (Py-IR) spectra were acquired on a Nicolet 380 spectrometer. Samples were pretreated under vacuum at 350 °C for 1 hour, cooled to 40 °C, and exposed to pyridine vapor for 10 min. After physisorbed pyridine removal, spectra were collected at room temperature and after desorption at 150 °C under dynamic vacuum.

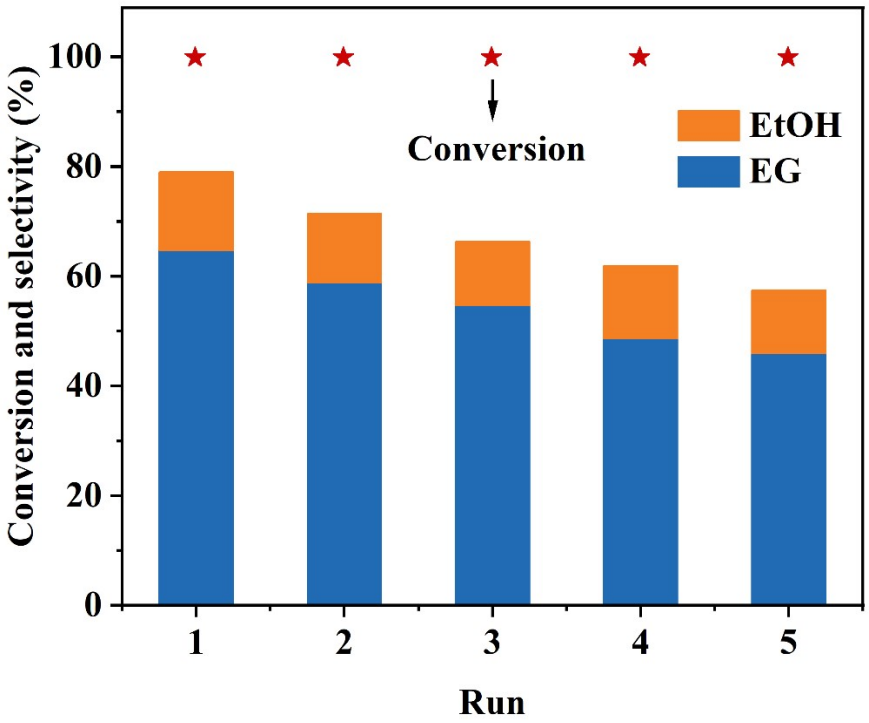

Fig. S1. Recycling tests of Ru/WNO-800. Reaction conditions: 0.1 g of cellulose, 0.05 g of catalysis, 30 mL of deionized water, 245 °C, initial 5 MPa H_2, 4 h. EG: ethylene glycol; EtOH: ethanol.

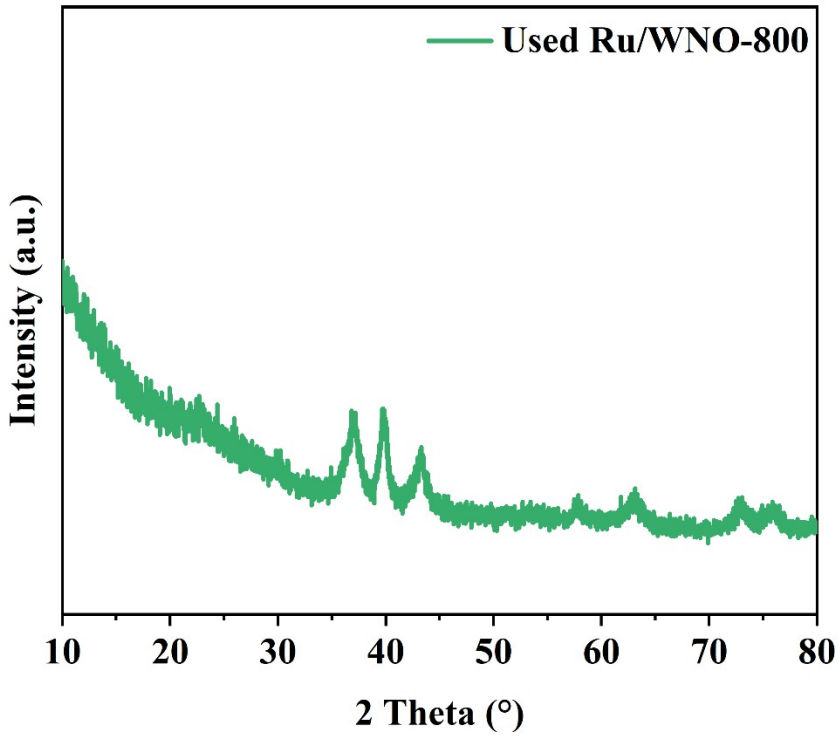

Fig. S2. XRD patterns of used Ru/WNO-800.

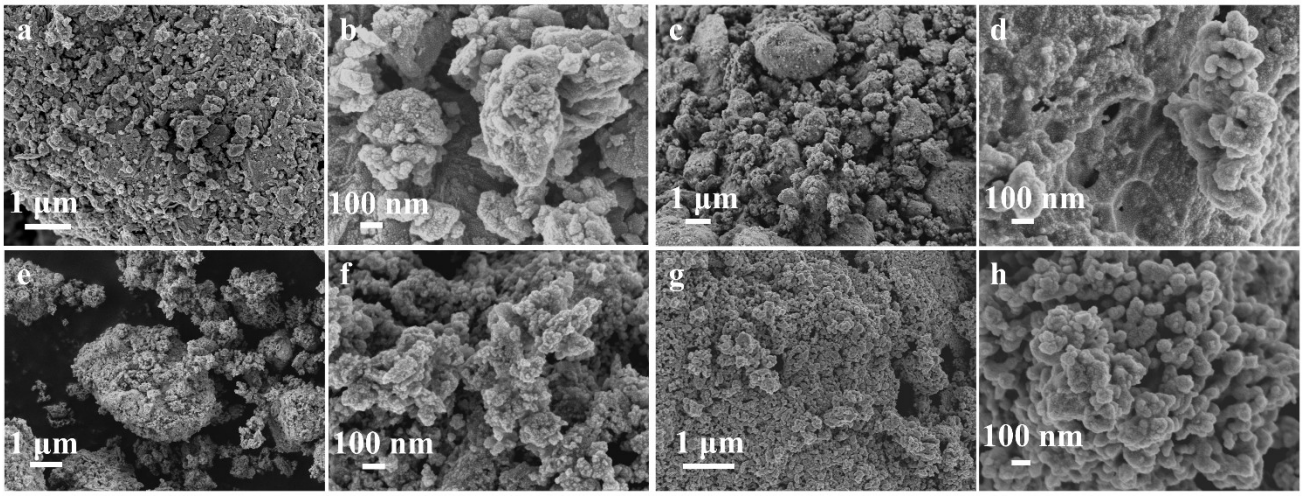

Fig. S3. SEM images of (a, b) Ru/WNO-400; (c, d) Ru/WNO-600; (e, f) Ru/WNO-800; (g, h) Ru/WNO-900.

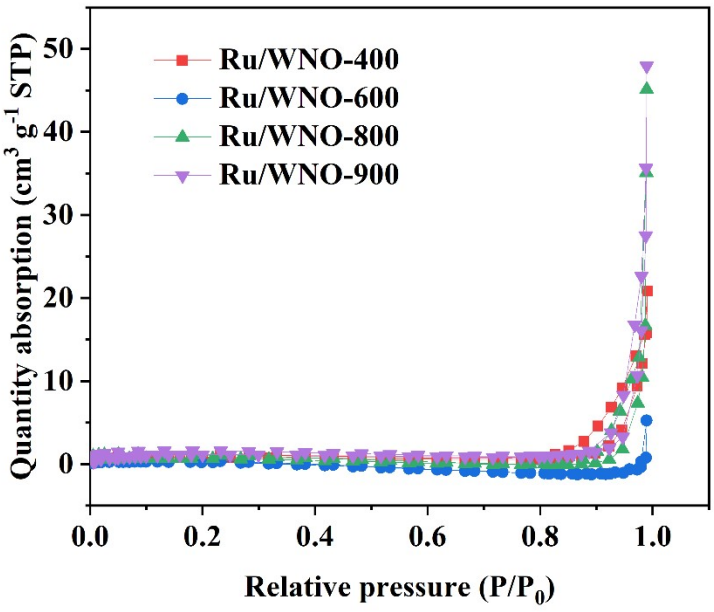

Fig. S4. N_2 adsorption–desorption isotherm of Ru/WNO-*t* catalysts.

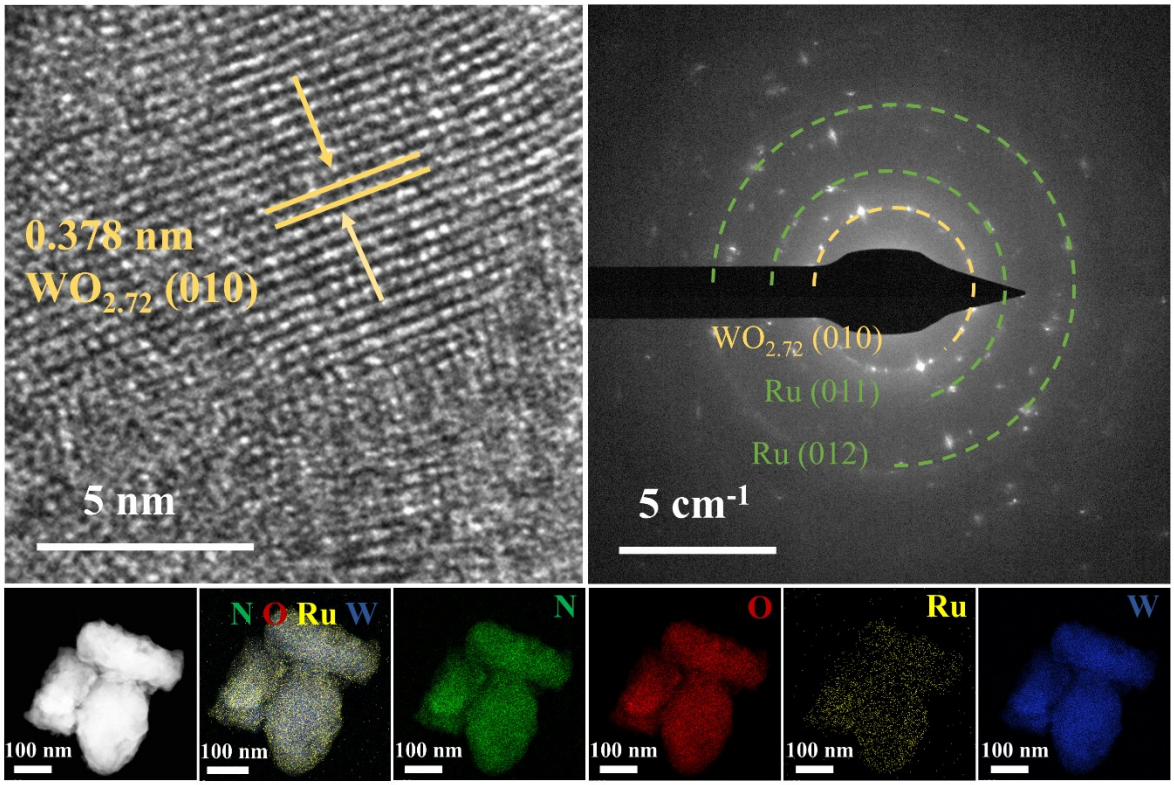

Fig. S5. TEM image, SAED pattern and elemental mapping images of Ru/WNO-400.

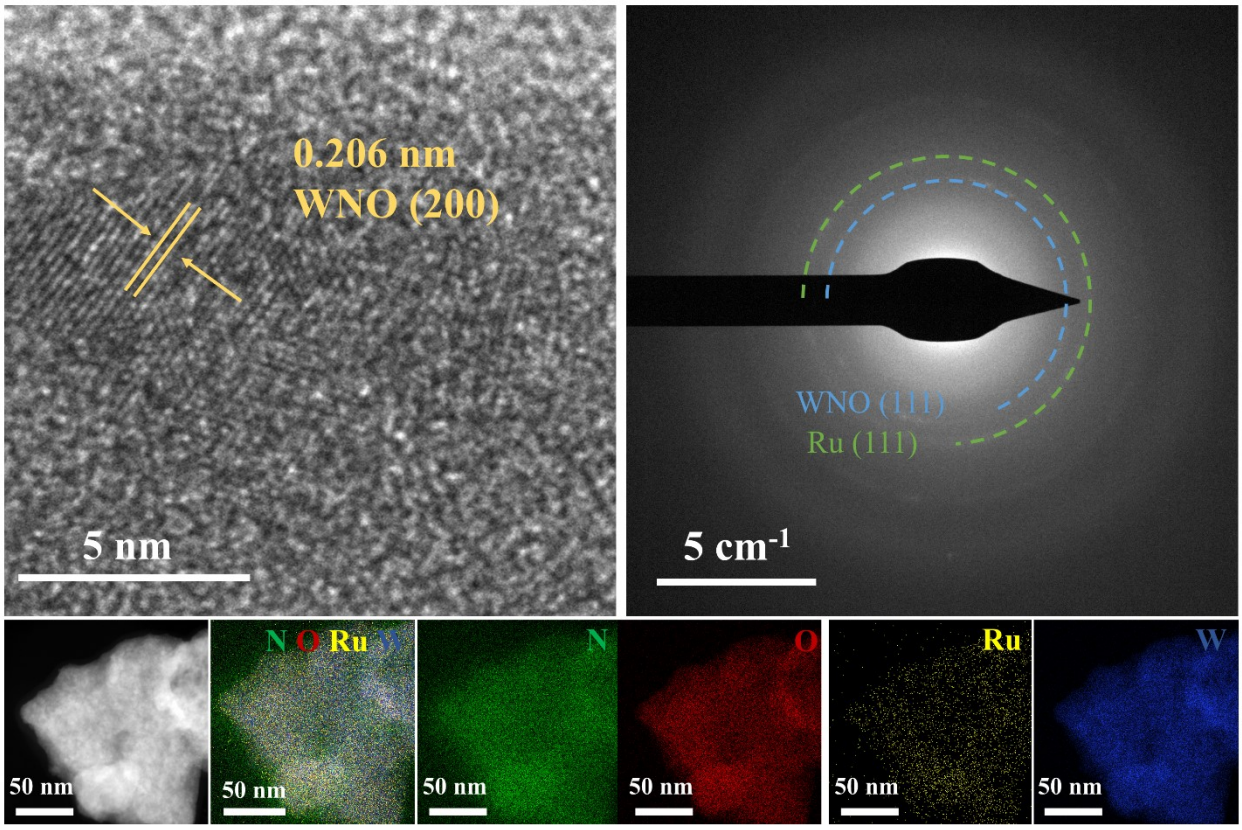

Fig. S6. TEM image, SAED pattern and elemental mapping images of Ru/WNO-600.

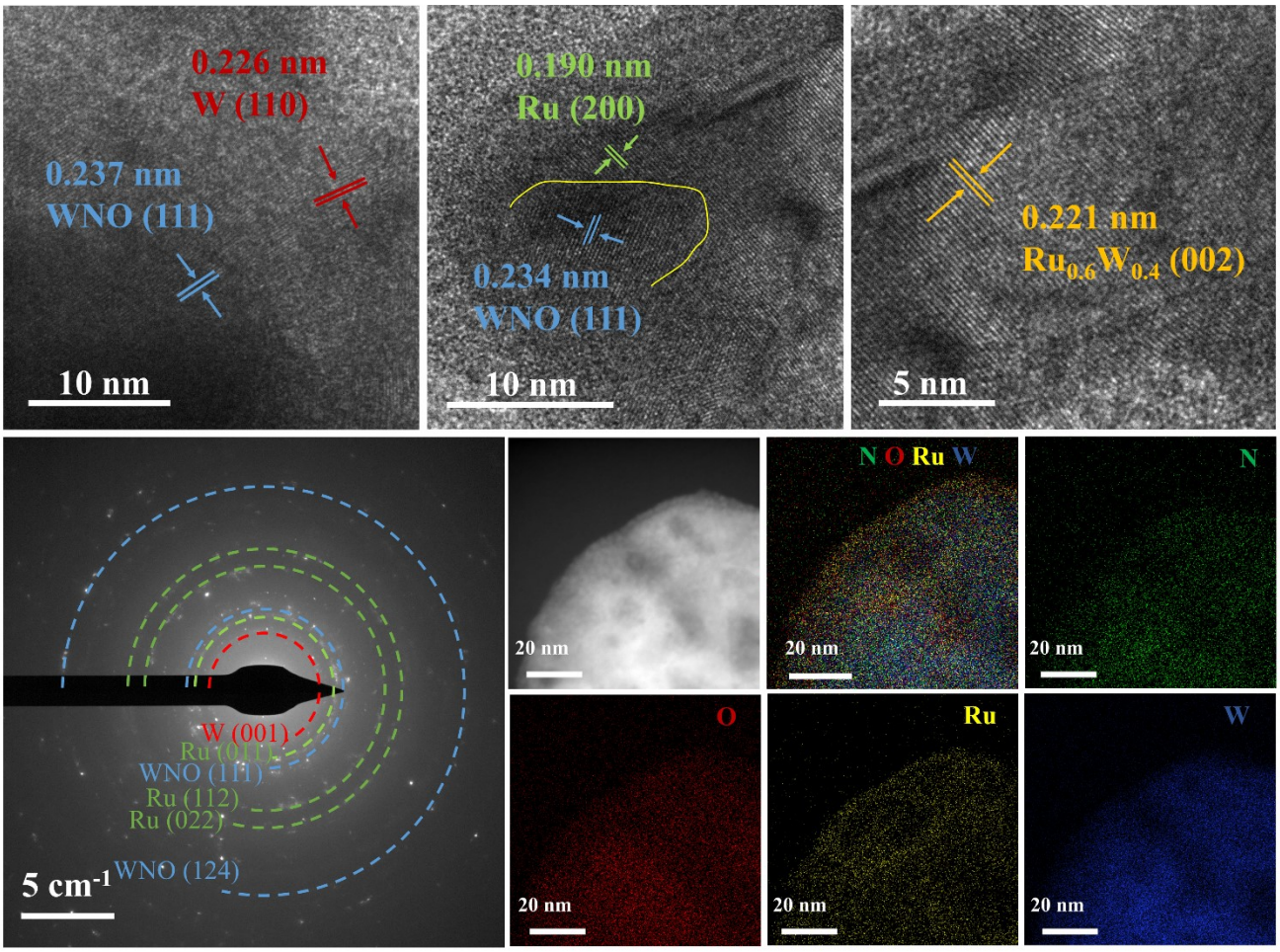

Fig. S7. TEM image, SAED pattern and elemental mapping images of Ru/WNO-900.

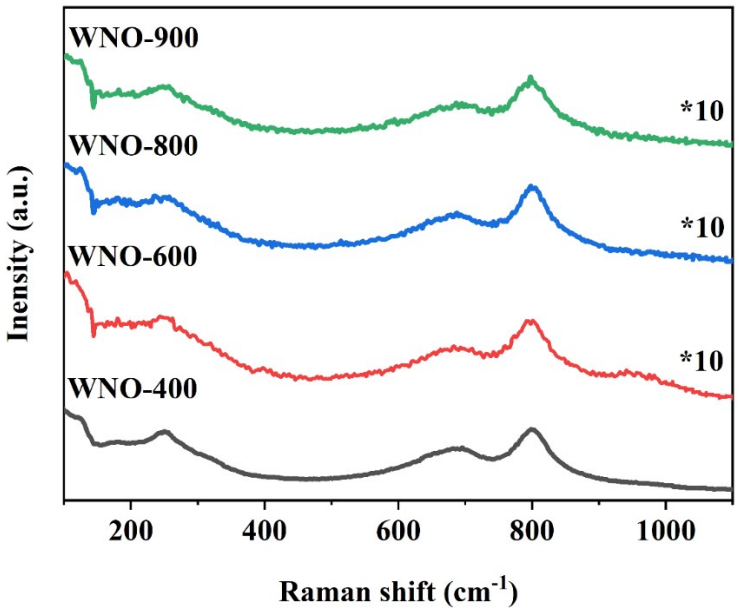

Fig. S8. Raman spectra of WNO-*t* catalysts.

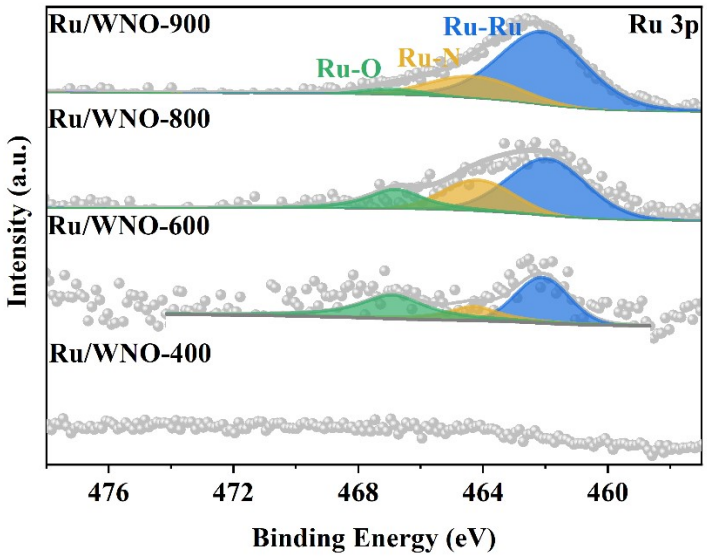

Fig. S9. Ru 3p spectra of Ru/WNO-*t* catalysts.

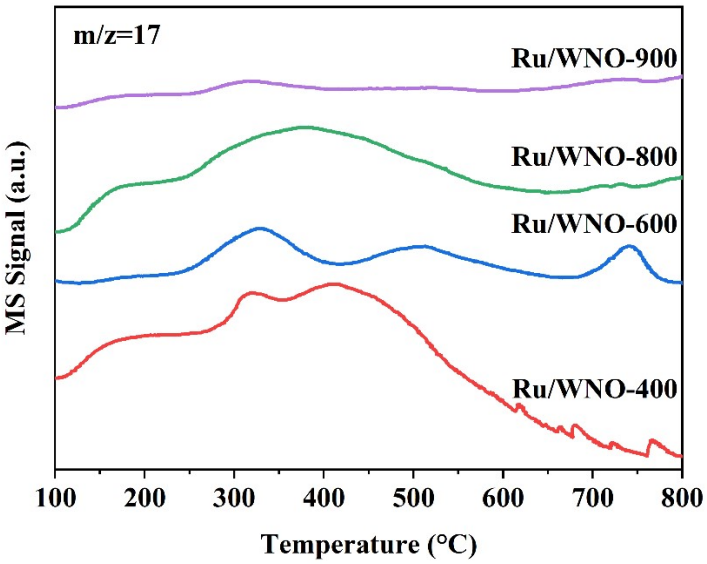

Fig. S10. NH_3-TPD profiles of Ru/WNO-*t* catalysts.

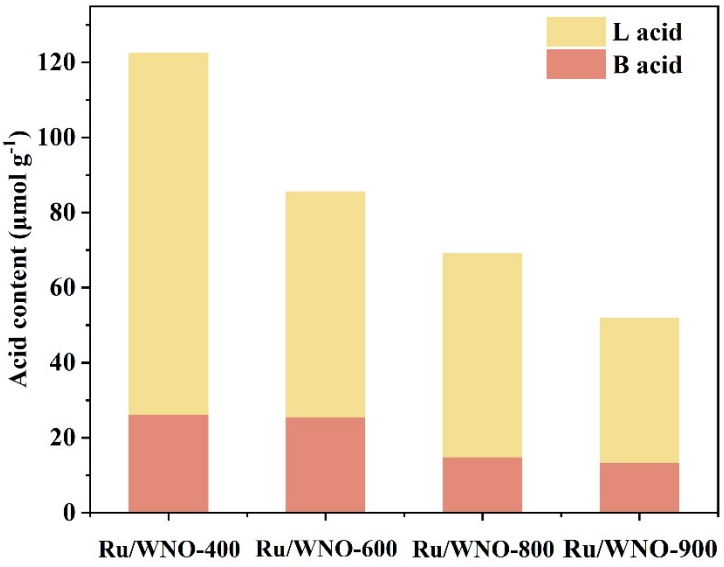

Fig. S11. Acidity content of Ru/WNO-*t* catalysts.

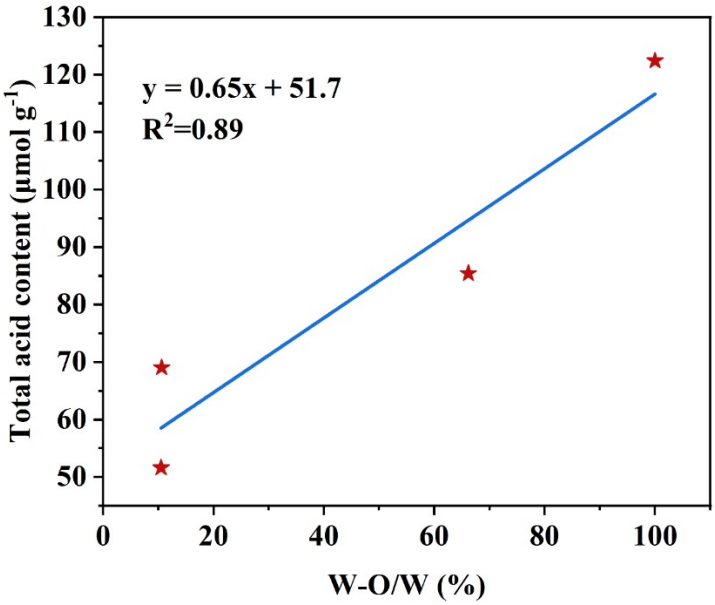

Fig. S12. The linear correlation between total acid amount and W-O bonds in Ru/WNO-*t* catalysts.

Table S1. Catalytic performance of Ru/WNO-*t*.

Catalysis	Conversion	Selectivity of products in liquid (%)							TOC
		Sor	Ery	EG	1,2-PG	1,2-BDO	EtOH	Others	
3Ru/WNO-400	>99	0.3	1.6	51.1	8.3	7.6	15.6	5.2	92.4
3Ru/WNO-600	>99	0.3	1.2	55.9	9.7	10.0	12.8	4.5	94.4
3Ru/WNO-800	>99	0.4	1.1	64.1	9.1	7.2	13.3	3.0	98.2
3Ru/WNO-900	>99	3.5	3.2	57.2	8.6	6.4	10.5	4.6	94.0

Reaction condition: 0.1 g cellulose, 0.05 g catalysts, 245 ℃, 5 MPa H_2, 4 h. EG: ethylene glycol; EtOH: ethanol; 1,2-PG: 1,2-propylene glycol; 1,2-BDO: 1,2-butanediol; Sor: sorbitol; Ery: erythritol. Others: LA, Formic acid, acetic acid and other unidentified polyols and oligomers. TOC means total organic carbon in the liquid product.

Table S2. Catalytic performance of previously reported catalysts.

Catalysts	Temperature /°C	Pressure /MPa	Time /h	EG /%	EtOH /%	References
$NiCu/WO_3$	245	5.5	4	58.9	3.9	[1]
$Ru\text{-}WOx/SiO_2$(500 Å)	240	4	5	51.5	5.1	[2]
$Ir\text{-}WOx/SiO_2$(500 Å)	280	4	5	0.4	40.5	
Ni-Cu/4ZnO-CNT	255	4	6	24	-	[3]
$NiW\text{-}[NC]\text{-}H_2$	245	6	1	51	-	[4]
$Ni@C/WO_x$	250	5	2	69.4	-	[5]
$Ru\text{-}WO_x$/TATP	245	5	3	62.9	-	[6]
$Pd/o\text{-}WO_3$	245	5.5	4	64.8	15.4	[7]
$Ru\text{-}WO_x/Nb_2O_5$	230	4	6	3.1	50.3	[8]
$Pt\text{-}WO_x/Nb_2O_5$				52.6	25.9	
Pd/WO_x	230	5	4	59.6	17.5	[9]

Table S3. Catalytic performance of Ru/WNO-800 under different reaction conditions.

Reaction conditions				Conversion	Selectivity of products in liquid (%)							TOC
Temperature (°C)	H_2 Pressure (MPa)	Time (h)	Ratio catalyst/cellulose	(%)	EG	EtOH	1,2-PG	1,2-BDO	Sor	Ery	Others	
215	5	4	1:2	71	30.0	7.6	5.6	6.4	1.5	3.2	6.6	60.9
230	5	4	1:2	>99	50.9	9.6	6.9	7.7	1.7	3.2	5.6	85.6
245	5	4	1:2	>99	64.1	13.3	9.1	7.2	0.4	1.1	3.0	98.2
260	5	4	1:2	>99	56.4	13.2	8.3	5.8	0.1	0.9	5.0	89.7
245	6	4	1:2	>99	57.7	11.4	5.0	8.1	0.7	2.4	1.0	86.3
245	4	4	1:2	>99	52.6	10.5	7.2	7.3	0.6	1.4	1.2	80.8
245	3	4	1:2	>99	48.4	10.4	4.7	5.8	0.3	1.3	0.5	71.4
245	5	5	1:2	>99	53.7	13.7	5.2	8.1	0.2	1.7	0.8	83.4
245	5	3	1:2	>99	57.4	9.4	12.3	6.6	3.0	3.3	0.5	92.5
245	5	2	1:2	>99	40.2	10.9	8.1	8.9	2.5	2.4	0.7	73.7
245	5	4	1:3	>99	52.9	10.0	7.0	6.4	1.3	1.7	4.3	83.6

EG: ethylene glycol; EtOH: ethanol; 1,2-PG: 1,2-propylene glycol; 1,2-BDO: 1,2-butanediol; Sor: sorbitol; Ery: erythritol. Others: LA, Formic acid, acetic acid and other unidentified polyols and oligomers. TOC means total organic carbon in the liquid product.

Table S4. The elemental content of Ru and W in the solution after reaction.

Catalysts	Ru (mg L^{-1})	W (mg L^{-1})
Ru/WNO-800	0.22	132.81

Table S5. Structural parameters of Ru/WNO-*t* catalysts.

Catalysts	Surface Area ($m^2\ g^{-1}$)	Mecopore Volume ($10^{-3}\ cm^3\ g^{-1}$)	Average Pore Diameter (nm)
Ru/WNO-400	3.19	1.09	34.50
Ru/WNO-600	1.15	1.04	16.48
Ru/WNO-800	2.64	1.23	65.81
Ru/WNO-900	4.43	0.55	64.66

Table S6. Relative acid amount of Ru/WNO-*t* catalysts obtained by NH_3-TPD curves.

Catalysts	Relative acid amount $\times 10^3$ (a.u.)
Ru/WNO-400	17.4
Ru/WNO-600	9.1
Ru/WNO-800	7.8
Ru/WNO-900	2.8

Table S7. Different acid types of Ru/WNO-*t* catalysts obtained by Py-IR spectra.

Catalysts	B acid	L acid	Total acid
Ru/WNO-400	26.1	96.3	122.4
Ru/WNO-600	25.4	60.0	85.4
Ru/WNO-800	14.9	54.1	69.0
Ru/WNO-900	13.5	38.2	51.6

Reference

1. X. Yang, Z. Li, M. Guo, T. Zhao, X. Su, W. Jiang, G. Han and H. Ben, *Fuel*, 2023, **341**, 127560.
2. Y. Weng, Y. Wang, M. Zhang, X. Wang, Q. Sun, S. Mu, H. Wang, M. Fan and Y. Zhang, *Catalysis Today*, 2023, **407**, 89-95.
3. H. Ma, C. v. d. Wijst, S. F. Morken and D. Chen, *Catalysis Today*, 2024, **435**, 114694.
4. J. Boulos, F. Goc, N. Perret, F. Rataboul, J. Dhainaut and S. Royer, *ACS Applied Nano Materials*, 2024, **7**, 16086-16096.
5. M. Chen, Z. Yang, H. Xin, Y. Wang, D. Liang and C. Li, *ACS Sustainable Chemistry & Engineering*, 2025, **13**, 15201-15213.
6. Y. Zhao, Y. Ju, B. Guo, P. Gan, P. Lv, J. Yang, C. Qiao and K. Zhang, *RSC Advances*, 2025, **15**, 34754-34767.
7. W. Jia, W. Liu, Y. Cui, H. Song, C. Zhou, W. Jiang, H. Ben, X. Yang and D. Chen, *Journal of Catalysis*, 2025, **442**, 115860.
8. D. Wu, Y. Liu, X. Zhang, J. Liu, Q. Zhang, L. Ma and L. Chen, *Applied Catalysis A: General*, 2025, **699**, 120275.
9. W. Jia, H. Song, D. Wang, C. Zhou, Y. Zhao, Y. Cui, H. Ben and X. Yang, *ACS Sustainable Chemistry & Engineering*, 2025, **13**, 13274-13283.